HHS Public Access

Author manuscript

Cell Rep. Author manuscript; available in PMC 2020 January 30.

Published in final edited form as:

Cell Rep. 2019 July 30; 28(5): 1127–1135.e4. doi:10.1016/j.celrep.2019.06.087.

Monocytes Acquire the Ability to Prime Tissue-Resident T Cells via IL-10-Mediated TGF-β Release

Elizabeth A. Thompson[1,2,7,*], **Patricia A. Darrah**[3], **Kathryn E. Foulds**[3], **Elena Hoffer**[1,2], **Alayna Caffrey-Carr**[4], **Sophie Norenstedt**[5], **Leif Perbeck**[6], **Robert A. Seder**[3], **Ross M. Kedl**[4], **Karin Loré**[1,2,8,*]

[1]Department of Medicine, Division of Immunology and Allergy, Karolinska Institutet and Karolinska University Hospital, Stockholm 17164, Sweden

[2]Center for Molecular Medicine, Karolinska Institutet, Stockholm 17176, Sweden

[3]Vaccine Research Center, NIAID, NIH, Bethesda, MD 20892, USA

[4]Department of Immunology & Microbiology, University of Colorado Denver, Aurora, CO 80045, USA

[5]Kirurgkliniken, Capio St Görans Sjukhus, Stockholm 11281, Sweden

[6]Department of Surgery, Karolinska University Hospital, Solna 17176, Sweden

[7]Present address: Bloomberg-Kimmel Institute for Cancer Immunotherapy, Johns Hopkins School of Medicine, Baltimore, MD 21231, USA

[8]Lead Contact

SUMMARY

Using non-human primates (NHPs), mice, and human primary cells, we found a role for interleukin-10 (IL-10) in the upregulation of the tissue-resident memory T cell (T_{RM}) marker CD103. In NHPs, intravenous, but not subcutaneous, immunization with peptide antigen and an adjuvant combining an agonistic anti-CD40 antibody plus poly(IC:LC) induced high levels of $CD103^+$ T_{RM}s in the lung, which correlated with early plasma IL-10 levels. Blocking IL-10 reduced CD103 expression on human T cells stimulated *in vitro* with the adjuvant combination as well as diminished CD103 on lung-resident T cells *in vivo* in mice. Monocyte-produced IL-10 induced the release of surface-bound transforming growth factor β (TGF-β), which in turn upregulated CD103 on T cells. Early TGF-β imprinted increased sensitivity to TGF-β

*Correspondence: ethomp58@jhmi.edu (E.A.T.), karin.lore@ki.se (K.L.).

AUTHOR CONTRIBUTIONS

E.A.T., R.A.S., R.M.K., and K.L. designed the research. E.A.T., P.A.D., K.E.F., E.H., and A.C.-C. performed experiments. E.A.T., P.A.D., R.A.S., R.M.L., and K.L. analyzed data. S.N. and L.P. provided human skin samples and scientific input. E.A.T. and K.L. wrote the paper with input from all authors.

DECLARATION OF INTERESTS

R.M.K. is a founder of ImmuRx, a vaccine company for which intellectual property is based on the combined Toll-like receptor (TLR) agonist and anti-CD40 immunization platform. The remaining authors declare no competing interests.

SUPPLEMENTAL INFORMATION

Supplemental Information can be found online at https://doi.org/10.1016/j.celrep.2019.06.087.

restimulation, indicating an early commitment of the T cell lineage toward T_{RM}s during the priming stage of activation. IL-10-mediated TGF-β signaling may therefore have a critical role in the generation of T_{RM} following vaccination.

Graphical Abstract

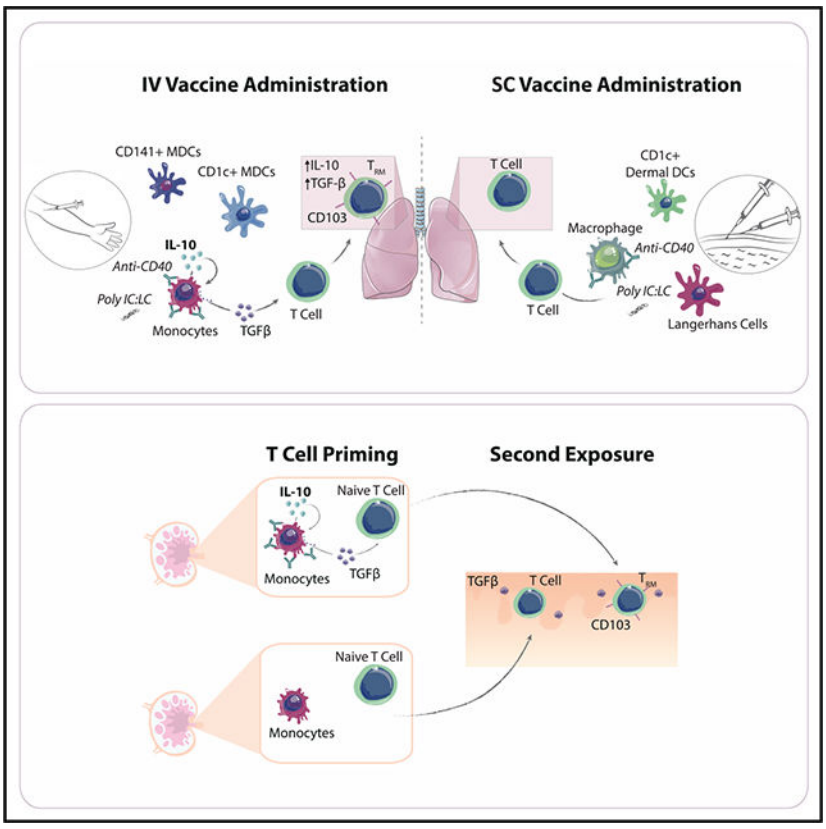

In Brief

Thompson et al. outline a role for early IL-10 following immunization in the release of TGF-β and subsequent differentiation of $CD103^+$ T_{RM}s. Using a combination of non-human primate, human, and murine systems, the authors demonstrate that blocking IL-10 reduces CD103 expression, whereas delivery of IL-10 can augment a $CD103^+$ phenotype.

INTRODUCTION

The majority of approved vaccines elicit antibody-mediated protection, yet there is a growing need for T-cell-based vaccines. The recently identified tissue-resident memory T cells (T_{RM}s) have been shown to play a central role in protection against infection and tumor clearance (Mueller and Mackay, 2016). T_{RM}s do not recirculate but instead are restricted to tissues, where they contribute to the frontline defense by mediating a variety of functions (Beura et al., 2018; Schenkel et al., 2013). There is an incomplete understanding of how to generate T_{RM}s through vaccination. Much of the work characterizing T_{RM}s has been performed in mice, which has important limitations. Standard laboratory mouse strains

inherently have limited pathogen exposure and subsequently more immature T cell populations (Beura et al., 2016). In contrast, non-human primates (NHPs) provide a more predictive model for humans to assess T_{RM}s and can be followed longitudinally after infection or vaccination (Pichyangkul et al., 2015; Thompson et al., 2015).

Immune stimulatory vaccine adjuvants provide a powerful tool to modulate the type of adaptive response a vaccine elicits by utilizing early innate immune activation and could therefore be used to educate T_{RM} development. We recently showed that an adjuvant combining an agonistic-CD40antibody (Ab) with the TLR3 ligand poly(IC:LC) elicited high levels of $CD103^+$ T_{RM}s largely restricted to the lungs of NHPs following intravenous (i.v.) administration (Thompson et al., 2015). This vaccine approach in NHPs therefore offers a uniquely translatable model to study the effects of antigen-presenting cell (APC) targeting and innate immune stimulation for T cell homing, development, and retention of T_{RM}s in mucosal tissues. We therefore utilized alternative routes of administration to selectively target APCs and understand the innate mechanisms affecting the T_{RM} phenotype in this *in vivo* model and discovered a role for interleukin-10 (IL-10) in the early education of the T cell phenotype.

RESULTS AND DISCUSSION

Differential *In Vivo* Innate Targeting via Alternative Routes of Administration

To investigate innate immune mechanisms that determine the induction of T_{RM}s, we established an *in vivo* model using rhesus macaques, where different sites and populations of APCs were targeted with the anti-CD40Ab and poly(IC:LC) adjuvant combination through i.v. or subcutaneous (s.c.) administration. The anti-CD40Ab was fluorescently labeled with Alexa Fluor 680 to determine the biodistribution and specific APC targeting after delivery (Figure 1A). As we reported earlier, i.v. administration resulted in dissemination of the anti-CD40Ab throughout many tissues (Thompson et al., 2015). In contrast, the Ab stayed highly localized after s.c. administration (Figure 1B) and was found predominantly in the skin of the injection site and the vaccine-draining axillary lymph node (LN), but not in any non-draining LNs (Figures 1C and 1D). Importantly, there was almost no detection of Ab into the blood at 6 or 24 h (Figure 1E) or the lungs (Figure 1F). Therefore, there was very limited potential for systemic targeting and activation by s.c. administration, in stark contrast to i.v. administration (Figure 1G). Macrophages and monocytes in the skin were the primary APCs targeted after s.c. administration (Figures 1B and 1C). In the skin, neutrophils also displayed high levels of CD40Ab binding, whereas B cells and T cells showed limited to no binding (Figure S1D). The *in vivo* findings were confirmed using *in vitro* cultures, demonstrating that primary rhesus and human APC subsets from blood and skin showed similar binding and uptake patterns of the the CD40Ab, where blood monocytes showed the highest level of internalization (Figures S1A–S1D). Together, this demonstrates that s.c. and i.v. administration efficiently targets local and systemic APCs, respectively.

Induction of Tissue-Resident T Cells following Intravenous Administration Correlates with Systemic IL-10 Production

To determine how systemic versus resident APCs influence vaccine-specific T cell homing to and retention in the lungs, rhesus macaques received a single immunization of anti-CD40Ab, poly(IC:LC), and HIV-1 envelope (Env) glycoprotein peptides via either the i.v. or s.c. route. Env peptides were used as a prototype antigen (Ag), since they are well characterized and highly immunogenic in rhesus macaques (Thompson et al., 2015; Nehete et al., 2008), which enabled us to focus on immune modulation. Since we have previously shown that vaccine-specific T cells were found almost exclusively in the lung and no other mucosal tissues following i.v. administration (Thompson et al., 2015), we focused on the induction of T cell homing to the lung. Peripheral blood mononuclear cells (PBMCs) and bronchoalveolar lavage (BAL) were evaluated at peak response (3 weeks) for Ag-specific T cells (Figures S2A and 2A). Both i.v. and s.c. delivery induced robust T cell responses in the BAL, and there were no significant differences between the groups in terms of quantity or multifunctionality (Figures 2A and 2B). Previous reports in mice have suggested that T cell responses in the lung are rapidly generated but short lived (Slütter et al., 2017). However, in rhesus macaques, well-detectable Ag-specific T cell responses were found in the BAL 9 months later (Figure 2C). Although the frequencies of Ag-specific CD4 and CD8 T cell responses had waned at this time, they correlated with the responses in the same animal at the peak response (Figure S2B). This demonstrates that both i.v. and s.c. immunization induced homing to the lungs, and animals that primed a strong T cell response maintained a higher pool of Ag-specific T cells in the lung over time. It is well documented that dendritic cells (DCs) from different tissues are capable of imprinting T cell homing (Mikhak et al., 2013; Mora et al., 2003); however, our results indicate that it is not strictly a matter of route of administration that dictates the T cell migration pattern. Indeed, Ag-specific T cells have been found in the lung following a variety of immunization routes (Darrah et al., 2014; Liu et al., 2010; Park et al., 2013). Lung homing may therefore be a universal outcome of many APC-T cell interactions, as the lung is highly vascularized and regularly exposed to environmental threats.

T_{RM}s have been phenotypically characterized through CD69 and CD103, with differences in tissue localization and possibly function depending on the phenotype. However, CD69 is an early activation marker that can also be expressed on circulating T cells and is upregulated during the Ag recall assay. We therefore focused on the induction of $CD103^+$ CD8 T cells, which represent a more homogeneous tissue-resident phenotype. Despite the similarities in T cell homing to the lung between the administration routes, there was a striking difference in the $CD103^+$ T_{RM} phenotype. Animals immunized i.v. had a significantly higher proportion of Ag-specific CD8 T cells that expressed CD103 (Figure 2D), and these cells expressed higher levels of CD103 (Figure 2E). Therefore, although both routes induced robust levels of Ag-specific T cells in the lung, i.v. administration induced a markedly stronger $CD103^+$ T_{RM} polarized phenotype.

Upon T cell entry into tissues, local signals such as cytokine production and Ag retention can induce tissue residence via the expression of CD103. T_{RM} differentiation has shown variable dependence on Ag availability (Casey et al., 2012; McMaster et al., 2018; Pizzolla

et al., 2017). Here, we focused on how the innate cytokine profile influences priming of a T_{RM} phenotype. We found that both routes induced robust cell mobilization from the circulation and cytokine production (Figures S2C–S2F). Multivariate correlative analysis identified IL-10 as the systemic cytokine with the strongest correlation with the T_{RM} phenotype (Figures S2F and S2G). IL-10 is pleotropic cytokine, produced by multiple cell types, and has a critical role in immune regulation. There was significantly higher IL-10 production in the i.v. group (Figure 2F), and both poly(IC:LC) and CD40 stimulation were required for production (Figure 2G). There was a strong correlation ($p = 0.0011$) between the plasma levels of IL-10 at 6 h post-immunization with the frequencies of Ag-specific T_{RM}s in the lung at 3 weeks post-vaccination, including all animals from both the i.v. and s.c. groups (Figure 2H). Although IL-10 may have been produced locally following s.c. immunization, only a limited amount reached the periphery and was detected in the plasma; therefore, any IL-10 in the s.c. group was unlikely to have an effect in the lung environment. IL-10 has previously been shown to be critical for CD8 memory formation; however, the induction of T_{RM}s was not addressed in these studies (Foulds et al., 2006; Laidlaw et al., 2015). Therefore, targeting innate cells to produce IL-10 could play an important role in the generation and maintenance of T_{RM}s.

Blood Monocytes Produce IL-10, Leading to Induction of the $CD8^+CD103^+$ T_{RM} Phenotype

To further investigate the effects of differential innate immune targeting and activation on the generation of primary T cell responses, we developed *in vitro* cell culture systems to identify mechanisms for T_{RM} priming. To represent the major cells targeted by i.v. or s.c. administration, primary APCs were sorted from human peripheral blood, epidermis, or dermis and stimulated *in vitro* with anti-CD40Ab and poly(I:C). Stimulated APCs were cultured with allogeneic purified naive T cells for 6 days to evaluate T cell priming and differentiation (Figure 3A). The stimulation significantly increased naive T cell proliferation when cultured with APCs from either blood or skin but had no effect on T cell proliferation in the absence of APCs, using instead CD3-CD28 bead activation (Figure 3B). However, similar to the *in vivo* findings, only stimulated blood APCs increased CD103 *in vitro* (Figure 3C). These data show that both blood and skin APCs are responsive to anti-CD40Ab and poly(I:C) treatment to increase T cell proliferation, but only blood APCs had the capacity to increase CD103 expression on CD8 T cells following stimulation.

Due to the strong correlation between plasma IL-10 levels and T_{RM}s in the lung, we characterized IL-10 production in relation to CD103 expression in the *in vitro* system. We found that APCs purified from blood, but not the skin, produced IL-10 in response to anti-CD40 and poly(I:C) stimulation, similar to the innate profiles seen after i.v. and s.c. administration *in vivo* (Figure 3D). Epidermal Langerhans cells and dermal DCs are either incapable of producing IL-10 or produce only low levels (Banchereau et al., 2012). In contrast, we found that of the blood APCs, monocytes produced the highest levels of IL-10 and did not promote bystander production of IL-10 within CD4 T cells (Figure S3). Since circulating monocytes were the primary target after i.v. administration and capable of producing IL-10 following adjuvant stimulation, blood APCs were used to directly test the contribution of IL-10 in T_{RM} development by culturing them with allogeneic naive T cells in the presence of a neutralizing anti-IL10 Ab or an isotype control Ab (Figure 3E). In

unstimulated conditions, the addition of a neutralizing IL-10 Ab had no effect on CD103 expression, likely due to the lack of IL-10 production. However, in the context of anti-CD40Ab and poly(I:C) stimulation, blocking IL-10 led to a significant reduction in CD103 expression. Conversely, directly adding recombinant IL-10 to unstimulated cultures increased CD103 expression, indicating that IL-10 is sufficient to induce CD103 expression (Figure 3F). Thus, the pathway described here should not be exclusive to adjuvants targeting CD40 and TLR3. APCs can, for example, also produce IL-10 in response to R848 (TLR7/8) and LPS (TLR4) (Cepika et al., 2017), which should be investigated for their ability to induce IL-10 and drive T_{RM} formation. However, the timing and level of IL-10 may be critical factors infiuencing the T cell response, since high concentrations of IL-10 can reduce T cell proliferation, in accordance with the inhibitory functions of IL-10 (Figure S3C). We found that IL-10 did not act directly on the T cells to modulate their CD103 expression, as adding recombinant IL-10 to T cells stimulated with anti-CD3-CD28 beads did not increase CD103 expression (Figure 3F). This suggests that IL-10 conditions APCs to induce the $CD103^+$ T_{RM} phenotype. Finally, these findings were confirmed in an *in vivo* mouse system, where blocking the IL-10 receptor at the time of immunization with anti-CD40, poly(I:C), and ovalbumin (OVA) reduced CD103 expression on lung-resident T cells (Figure 3G). This highlights not only the *in vivo* relevance of IL-10 in upregulation of CD103 but also the conserved nature of this pathway among humans, NHPs, and mice.

IL-10 Mediates TGF-β Release to Prime T_{RM}

There is a well-characterized role for transforming growth factor β (TGF-β), originating from tissue microenvironments or immune cells, in CD103 upregulation (Casey et al., 2012; Mackay et al., 2013, 2015; Yu et al., 2013). APCs stimulated with anti-CD40Ab and Poly I:C produced elevated levels of TGF-β1 in culture supernatants, which was inhibited with a neutralizing anti-IL-10 Ab (Figure 4A). Further, adding recombinant IL-10 to APCs mediated the release of TGF-β1 (Figure 4B). Therefore IL-10 is able to condition APCs to secrete TGF-β. APCs also express surface-bound TGF-β, which has been suggested to induce CD103 on T cells (Yu et al., 2013). Monocytes expressed significantly higher levels of surface TGF-β than DC subsets (Figure 4C), and stimulation with anti-CD40Ab and poly(I:C) significantly reduced surface expression of TGF-β (Figure 4D). The levels of TGF-β released in the supernatant of bulk APCs significantly correlated with a decrease in monocyte surface TGF-β expression (Figure 4E). This was not the case for $CD1c^+$ myeloid dendritic cells (MDCs), likely due to their lower expression of TGF-β and the lower frequency (Figures S4A and S4B). As monocytes express the highest level of the IL-10 receptor among circulating leukocytes (von Haehling et al., 2015), they could consume IL-10 in an autocrine fashion following stimulation, leading to the release of TGF-β. These results indicate that in response to stimulation, monocytes released surface TGF-β, providing a potential mechanism for the increase CD103 expression on T cells.

To determine if monocytes were sufficient to induce CD103 on T cells due to their high production of both IL-10 and TGF-β, $CD14^+$ monocytes were purified and cultured with allogeneic naive T cells (Figure 4F). Monocytes increased the expression of CD103 on T cells in the absence of DCs. We found that this effect could be mediated by soluble factors, as transwell experiments or transferring supernatants from stimulated $CD14^+$ monocytes to

CD3-CD28 stimulated naive T cells generated the same results (Figure 4G). However, the effect was more pronounced in cultures that allowed for direct cell-to-cell contact and interaction with soluble factors, indicating there may also be a role for activated surface-bound TGF-β in addition to the secreted form, as suggested previously for $CD1c^+$ MDCs (Yu et al., 2013). Therefore, monocytes are unique in their ability not only to produce high levels of IL-10 but also to release surface-bound TGF-β following stimulation to modulate T cell CD103 expression. In contrast, $CD1c^+$ MDCs were superior at inducing both T cell proliferation and CD103 expression at baseline and were therefore less responsive to stimulation (Figures S4C and S4D). Although monocytes are inferior at priming naive T cell responses (Vono et al., 2017), DCs are rare populations in comparison and only represent a minority of cells targeted directly with vaccination (Liang et al., 2017; Thompson et al., 2015). Instead, monocytes are highly abundant in the blood and often the primary subset recruited into the site of vaccination (Liang et al., 2017). Monocytes therefore offer an expanded pool of target APCs that are capable of inducing CD103 expression following vaccine exposure, and the contribution of a large population of adjacent monocytes may be central for increasing the CD103 expression on T cells above basal levels.

Although TGFβ has been well characterized for upregulation of CD103, it has been unclear if priming and bifurcation of T cells based on signals received in the LN could imprint future tissue residence. Since IL-10 and TGF-β were produced within 6 h of stimulation, the early kinetics suggested that the role of IL-10 in promoting tissue residence may occur during the initial priming in the LN instead of upon reentry of the T cell into the tissue several days later. By adding recombinant TGF-β to proliferating naive T cells on different days of the culture, we found that T cells exposed to TGF-β from the start upregulated CD103 to the highest extent (Figure 4H). In contrast, TGF-β added on day 5 did not upregulate CD103 within 1 day. This indicates that CD103 upregulation can occur over several days and that early priming in the presence of TGF-β may be critical for subsequent upregulation in the tissue. We tested if T cells that had been primed in the presence of TGF-β but had not upregulated CD103 were more responsive to subsequent TGF-β exposure (Figure 4I). To mimic priming in a LN, naive T cells were exposed to TGF-β for 3 days and then washed and rested for 2 days. $CD103^-$ T cells were then sorted and restimulated with TGF-β, simulating entry into a tissue microenvironment. Newly upregulated CD103 was evaluated after an additional day of culture. Despite a high purity of the sorted $CD103^-$ cells, T cells primed in the presence of TGF-β continued to upregulate CD103 over the following day, indicating delayed kinetics of expression (Figure 4J). Additionally, these cells could further augment their CD103 expression with the addition of TGF-β. In contrast, T cells that had not experienced TGF-β during the priming on day 0 showed little upregulation of CD103 with or without the late TGF-β exposure (Figure 4J).

Early priming of T cells in the presence of IL-10 and TGF-β may therefore allow them to upregulate CD103 over several days after entry to the tissue and imprint them to become more responsive to a TGF-β tissue environment, as summarized in Figure 4K. Since blood monocytes are rapidly recruited into vaccine draining LNs (Liang et al., 2017), they should be able to produce IL-10 and TGF-β locally following stimulation to influence naive T cell priming. Had T_{RM}s been evaluated in the skin following s.c. immunization, it is possible

they would correlate with locally produced IL-10, which is not detectable in the plasma. This would be important to evaluate in future studies.

Together, our data suggest that i.v. delivery of anti-CD40 and poly(IC:LC) would be a potent combination for lung cancer or infectious diseases requiring lung-resident T_{RM}s, such as tuberculosis, influenza, or respiratory syncytial virus. Further, we have also discovered a more general role for IL-10 in the development of T_{RM}s; therefore, these findings could be important for alternative adjuvants that induce IL-10 or the use of recombinant IL-10 directly. Although still early in development, it is highly promising that recombinant IL-10 has already shown evidence of antitumor activity through CD8 T cell activation in humans and mice (Mumm et al., 2011; Naing et al., 2016). Although T cells have not been evaluated for a T_{RM} phenotype following IL-10 treatment, there was increased CD8 T cell activation and infiltration into the tumor. Since improved prognosis has been correlated with tumor-associated T_{RM}s (Ganesan et al., 2017; Nizard et al., 2017; Savas et al., 2018), it is tempting to speculate that IL-10 could also be driving increased T_{RM} formation in these patients. These results may at first seem counterintuitive, as IL-10 has classically been thought of as a highly immune-suppressive cytokine; however, a growing body of literature suggests that IL-10 may in fact be critical for Th1 cell function and memory formation. Our study further contributes to the developing consensus on the pleiotropic nature of IL-10 and outlined a mechanism for IL-10 to contribute to CD8 T cell memory and tissue retention, which is likely critical for the clinical success of cancer immunotherapies. Therefore, direct application of recombinant IL-10 or targeting monocytes to produce low levels of IL-10 systemically or at specific sites may be a strategy to optimize vaccine-induced T_{RM}s and T cell activation.

STAR★METHODS

LEAD CONTACT AND MATERIALS AVAILABILITY

Further information and requests for resources and reagents should be directed to and will be fulfilled by the Lead Contact, Karin Loré (Karin.lore@ki.se).

EXPERIMENTAL MODEL AND SUBJECT DETAILS

Human subjects—The work on human sample material was approved by the Institutional Review Board of Ethics (Stockholm, Sweden). Signed informed consent was obtained in accordance with the Declaration of Helsinki. All samples were not associated with any features that could be linked to identification, including sex and age. Sample size are indicated in relevant figure legends.

Rhesus macaques—Approval for the animal studies was granted by the Animal Care and Use Committees of the Vaccine Research Center, National Institutes of Health (NIH). Indian rhesus macaques were housed in pairs at Bioqual and handled according to the standards of the American Association for the Accreditation of Laboratory Animal Care. Animals were distributed evenly through groups based on sex (both male and female used), age, and weight. For tracking studies animals were 3–4 years old and for immunization studies animals were 14–16 years old. Sample size are indicated in relevant figure legends.

Mouse models—Approval for the animal studies was granted by the Animal Care and Use Committees of the University of Colorado, Denver. Female C57BL/6J mice used were aged 8 to 10 weeks old, group-housed at a temperature range of 21°to 23°C, with a 14-hour on and 10-hour off light cycle, and fed an irradiated standard diet (2920X; Envigo). Sample size are indicated in relevant figure legends.

METHOD DETAILS

Immunizations—Rhesus macaques received intravenous or subcutaneous administration of 1.5mg/kg αCD40Ab (clone 341G2 IgG2), 1mg poly(IC:LC) (Oncovir), and 1mg/kg HIV-1 Env peptides (Thompson et al., 2015; Nehete et al., 2008) (Biomatik). The Env peptides were resuspended to 50mg/ml in 30% DMSO prior to immunization. For Ab tracking studies, αCD40Ab was first conjugated to Alexa680 according to manufacturer's protocol (Molecular Probes) and delivered with poly(IC:LC).

Rhesus tissue and blood sample processing—Blood PBMCs were isolated using a density-gradient with Ficoll-Paque (GE Healthcare) according to standard procedures. All tissue samples were collected at euthanasia and processed to a single cell suspension following standard protocol. Briefiy; LN samples were manually disrupted and filtered through a 70um cell strainer. Skin tissues were incubated in 26 WU/ml Liberase (Roche) and 20 U/ml DNase I (Roche) in a gently shaking incubator (80rmp) at 37°C for 1h. Following digestion, the cell suspensions were collected and washed with RPMI 1640/5 U/ml DNase I and filtered through a 40-μm cell strainer. PBMCs and single cell suspensions were washed and maintained in complete media (R10; RPMI 1640/10% FCS/100 U penicillin/0.1 mg streptomycin; Sigma-Aldrich).

Antigen recall assay—For assessment of Ag-specific cytokine production, PBMCs or single cell suspensions for tissues were restimulated *in vitro*. 1.5×10^6 cells were cultured in 200ul of R10 per stimulation in a 96 well plate. Samples were stimulated with 2ug/ml immunizing peptides in the presence of 10 μg/ml brefeldin A (Sigma) overnight. Cells were first stained with LIVE/DEAD Fixable AquaBlue viability dye (Invitrogen) then surface stained and intracellularly stained (Table S1).

Rhesus phenotypic analysis—For innate studies and Ab dissemination studies, 6–24 hours following immunization, 5×10^6 cells were stained with LIVE/DEAD Fixable AquaBlue viability dye (Invitrogen) and blocked with FcR-blocking reagent (Miltenyi). Samples were then surfaced stained with a panel of fluorescently labeled Abs (Table S1) to determine cell distribution and maturation.

Cytokine secretion analysis—Rhesus plasma samples were evaluated for cytokine production using a custom NHP cross-reactive multiplex kit (EMD Millipore). ELISAs for IL-10 (Mabtech) and TGFβ−1 (R&D systems) were performed according to manufacturer's protocol. Samples were activated with 1N HCL and neutralized with 1.2N NaOH/0.5M HEPES using Sample Activation Kit (R&D systems) prior to TGFβ−1 ELISA, activated R10 levels were subtracted from all samples.

Isolation of blood APCs—APCs were enriched in blood from apheresed healthy donors by using a custom RosetteSep monocyte enrichment kit to deplete CD2, CD3, CD8, CD19, CD56, and CD66b (StemCell Technologies, custom kit catalog #15309) according to manufacturers protocols. Cells were then washed and cultured at 1×10^6 cells/ml at 37°C in R10. For cell sorting experiments, monocytes were further purified using positive selection CD14 microbeads. CD1c+ MDCs were purified from the negative fraction after CD14+ selection and CD19 microbead depletion, using CD1c-biotin followed by anti-biotin beads (Miltenyi). All separations were performed using an autoMACs (Miltenyi).

Isolation of human skin APCs—Skin samples were obtained from patients undergoing breast reconstruction surgery (Karolinska University Hosptial, Stockholm, Sweden), and primary APCs were isolated as previously published (Bond et al., 2009). Briefiy, skin pieces were sliced into nets using a skin graft mesher (Zimmer) then incubated in 2U/ml Dispase (Life Technologies) overnight at 4°C. The epidermis could then readily be separated from the dermis. Each fraction was incubated in 26 WU/ml Liberase (Roche) and 20 U/ml DNase I (Roche) in a gently shaking incubator (80rmp) at 37°C for 1h. Following digestion, the cell suspensions were collected and washed with RPMI 1640/5 U/ml DNase I and filtered through a 40-μm cell strainer.

***In vitro* anti-CD40Ab binding and APC stimulation—**RosetteSep enriched APCs or skin isolated APCs were cultured at 37°C or 4°C as indicated with 1ug/ml anti-CD40Ab or alexa-680 anti-CD40Ab (Clone 341G2) and/or 5ug/ml Poly I:C (Invivogen). Anti-CD40 binding was quantified as Alexa680 mean fluorescence intensity (MFI) with fluorescence minus one (FMO) levels subtracted for each cell subset. For APC activation, unconjugated anti-CD40Ab was used.

T cell stimulation—RosetteSep enriched APCs or skin isolated APCs were stimulated with anti-CD40/Poly I:C as described above for 1 hour. Naive T cells were sorted from an allogenic donor using naive T cell isolation beads (Miltenyi) and an autoMACs (Miltenyi). Naive T cells were labeled with CFSE (Life Technologies) according to standard protocols. T cells were then added to stimulated unwashed APCs in a 5:1 ratio and incubated for 6 days before staining for flow cytometry (Table S1). Alternatively, T cells were stimulated using the T cell activation/expansion kit containing beads coated with antibodies against CD2, CD3, and CD28 (Miltenyi). For transwell experiments, purified monocytes were cultured in the upper chamber and T cells stimulated with T cell activation/expansion kit in the lower chamber in a 1:5 ratio using a 24-well plate with polycarbonate membrane inserts (Corning). Where indicated, APCs were pre-incubated with a 5ug/ml neutralizing anti-IL10 (clone JES3–19F1, BD Biosciences) or isotype (clone R35–95, BD Biosciences) for 1 hour prior to anti-CD40/poly(I:C) stimulation. For IL-10 add-in experiments, recombinant IL-10 (Peprotech) was added directly to cultures. A dose of 250 pg/ml IL-10 was determined by titration.

***In vivo* IL-10R blocking—**Wild-type B6 mice were immunized IV with poly(I:C)/anti-CD40Ab/ovalbumin (40ug/40ug/100ug), with or without simultaneous IP injection of blocking αIL-10R antibody (1.5mgs, clone 1b1.3a, BioXcell). Ten days later mice were

injected IV with 2ug antiCD45-PEcy7 to label all cells within the vasculature. Ten minutes after IV antibody injection, the mice were sacrificed, the lungs removed and collagenase digested and then ficolled to enrich for lymphocytes. Pre and post ficoll samples were stained (to insure ficoll had not enriched for specific T cell populations) with antibodies against CD8, B220, CD69, CD103, and a live/dead discriminating dye, followed by FACS analysis using the Beckman Coulter Cytofiex. Cells were gated to exclude dead, B220+, and CD45 PEcy7+ cells, identifying only the CD8s residing within the lung parenchyma. Significance was tested using an unpaired two-tailed t test.

IL-10 secretion assay—RosetteSep enriched APCs were stimulated with anti-CD40Ab/poly(I:C) as described above for 1 hour. Naive T cells were sorted from an allogenic donor using naive T cell isolation beads (Miltenyi) and an autoMACs (Miltenyi). T cells were then added to stimulated unwashed APCs in a 5:1 ratio. After 6 or 24 hours of culture, IL-10 was captured on the surface of producing cells for 45 minutes using the IL-10 Secretion Assay according to manufacture's protocol (Miltenyi) and stained for flow cytometry (Table S1).

TGFβ expression—RosetteSep enriched APCs were stimulated with anti-CD40Ab and Poly I:C or recombinant IL-10 (Peptrotech) for 6 hours. IL-10 concentration was determined by titration at levels 5 times higher than MLR to account for increased consumption by APCs. Supernatants were collected for ELISA and cells were stained for flow cytometry (Table S1).

Multiparameter flow cytometry—Samples were resuspended in 1% paraformaldehyde before acquisition using a Fortessa flow cytometer or modified Fortessa X-50 (BD Biosciences).

QUANTIFICATION AND STATISTICAL ANALYSIS

Statistical calculations were performed in GraphPad Prism 6. As indicated in figure legends, data are shown as mean ± SEM and each dot represents a unique animal or donor unless otherwise noted. Data was tested for normality using GraphPad Prism 6 D'Agostino & Pearson omnibus normality test. Comparison between conditions were performed using two-tailed Student's t test (for comparison of two groups) or one-way ANOVA with Tukey's multiple comparison test (for comparison of multiple groups). Correlation analysis was performed using Spearman's test with two-tailed p value. A p value less than 0.05 was considered significant. Details of statistical tests used can be found in the figure legends.

Supplementary Material

Refer to Web version on PubMed Central for supplementary material.

ACKNOWLEDGMENTS

The authors thank John-Paul Todd (Vaccine Research Center, NIH) and the animal care personnel at Bioqual and Oncovir for providing poly(IC:LC). K.L. is supported by grant from Vetenskapsrådet (2015–02608). E.A.T. is supported by an intramural PhD salary grant from Karolinska Institutet as well as Fernström Foundation and the Swedish Society for Medical Research.

REFERENCES

Banchereau J, Thompson-Snipes L, Zurawski S, Blanck J-P, Cao Y, Clayton S, Gorvel J-P, Zurawski G, and Klechevsky E (2012). The differential production of cytokines by human Langerhans cells and dermal CD14(+) DCs controls CTL priming. Blood 119, 5742–5749. [PubMed: 22535664]

Beura LK, Hamilton SE, Bi K, Schenkel JM, Odumade OA, Casey KA, Thompson EA, Fraser KA, Rosato PC, Filali-Mouhim A, et al. (2016). Normalizing the environment recapitulates adult human immune traits in laboratory mice. Nature 532, 512–516. [PubMed: 27096360]

Beura LK, Mitchell JS, Thompson EA, Schenkel JM, Mohammed J, Wijeyesinghe S, Fonseca R, Burbach BJ, Hickman HD, Vezys V, et al. (2018). Intravital mucosal imaging of $CD8^+$ resident memory T cells shows tissue-autonomous recall responses that amplify secondary memory. Nat. Immunol 19, 173–182. [PubMed: 29311694]

Bond E, Adams WC, Smed-Sörensen A, Sandgren KJ, Perbeck L, Hofmann A, Andersson J, and Loré K (2009). Techniques for time-efficient isolation of human skin dendritic cell subsets and assessment of their antigen uptake capacity. J. Immunol. Methods 348, 42–56. [PubMed: 19576898]

Casey KA, Fraser KA, Schenkel JM, Moran A, Abt MC, Beura LK, Lucas PJ, Artis D, Wherry EJ, Hogquist K, et al. (2012). Antigen-independent differentiation and maintenance of effector-like resident memory T cells in tissues. J. Immunol 188, 4866–4875. [PubMed: 22504644]

Cepika A-MM, Banchereau R, Segura E, Ohouo M, Cantarel B, Goller K, Cantrell V, Ruchaud E, Gatewood E, Nguyen P, et al. (2017). A multi-dimensional blood stimulation assay reveals immune alterations underlying systemic juvenile idiopathic arthritis. J. Exp. Med 214, 3449–3466. [PubMed: 28935693]

Darrah PA, Bolton DL, Lackner AA, Kaushal D, Aye PP, Mehra S, Blanchard JL, Didier PJ, Roy CJ, Rao SS, et al. (2014). Aerosol vaccination with AERAS-402 elicits robust cellular immune responses in the lungs of rhesus macaques but fails to protect against high-dose Mycobacterium tuberculosis challenge. J. Immunol 193, 1799–1811. [PubMed: 25024382]

Foulds KE, Rotte MJ, and Seder RA (2006). IL-10 is required for optimal CD8 T cell memory following Listeria monocytogenes infection. J. Immunol 177, 2565–2574. [PubMed: 16888018]

Ganesan A-PP, Clarke J, Wood O, Garrido-Martin EM, Chee SJ, Mellows T, Samaniego-Castruita D, Singh D, Seumois G, Alzetani A, et al. (2017). Tissue-resident memory features are linked to the magnitude of cytotoxic T cell responses in human lung cancer. Nat. Immunol 18, 940–950. [PubMed: 28628092]

Laidlaw BJ, Cui W, Amezquita RA, Gray SM, Guan T, Lu Y, Kobayashi Y, Flavell RA, Kleinstein SH, Craft J, and Kaech SM (2015). Production of IL-10 by CD4(+) regulatory T cells during the resolution of infection promotes the maturation of memory CD8(+) T cells. Nat. Immunol 16, 871–879. [PubMed: 26147684]

Liang F, Lindgren G, Sandgren KJ, Thompson EA, Francica JR, Seubert A, De Gregorio E, Barnett S, O'Hagan DT, Sullivan NJ, et al. (2017). Vaccine priming is restricted to draining lymph nodes and controlled by adjuvant-mediated antigen uptake. Sci. Transl. Med 9, eaal2094. [PubMed: 28592561]

Liu L, Zhong Q, Tian T, Dubin K, Athale SK, and Kupper TS (2010). Epidermal injury and infection during poxvirus immunization is crucial for the generation of highly protective T cell-mediated immunity. Nat. Med 16, 224–227. [PubMed: 20081864]

Mackay LK, Rahimpour A, Ma JZ, Collins N, Stock AT, Hafon M-LL, Vega-Ramos J, Lauzurica P, Mueller SN, Stefanovic T, et al. (2013). The developmental pathway for CD103(+)CD8+ tissue-resident memory T cells of skin. Nat. Immunol 14, 1294–1301. [PubMed: 24162776]

Mackay LK, Wynne-Jones E, Freestone D, Pellicci DG, Mielke LA, Newman DM, Braun A, Masson F, Kallies A, Belz GT, and Carbone FR (2015). T-box transcription factors combine with the cytokines TGF-β and IL-15 to control tissue-resident memory T cell fate. Immunity 43, 1101–1111. [PubMed: 26682984]

McMaster SR, Wein AN, Dunbar PR, Hayward SL, Cartwright EK, Denning TL, and Kohlmeier JE (2018). Pulmonary antigen encounter regulates the establishment of tissue-resident CD8 memory T cells in the lung airways and parenchyma. Mucosal Immunol. 11, 1071–1078. [PubMed: 29453412]

Mikhak Z, Strassner JP, and Luster AD (2013). Lung dendritic cells imprint T cell lung homing and promote lung immunity through the chemokine receptor CCR4. J. Exp. Med 210, 1855–1869. [PubMed: 23960189]

Mora JR, Bono MR, Manjunath N, Weninger W, Cavanagh LL, Rosemblatt M, and Von Andrian UH (2003). Selective imprinting of gut-homing T cells by Peyer's patch dendritic cells. Nature 424, 88–93. [PubMed: 12840763]

Mueller SN, and Mackay LK (2016). Tissue-resident memory T cells: local specialists in immune defence. Nat. Rev. Immunol 16, 79–89. [PubMed: 26688350]

Mumm JB, Emmerich J, Zhang X, Chan I, Wu L, Mauze S, Blaisdell S, Basham B, Dai J, Grein J, et al. (2011). IL-10 elicits IFNγ-dependent tumor immune surveillance. Cancer Cell 20, 781–796. [PubMed: 22172723]

Naing A, Papadopoulos KP, Autio KA, Ott PA, Patel MR, Wong DJ, Falchook GS, Pant S, Whiteside M, Rasco DR, et al. (2016). Safety, antitumor activity, and immune activation of pegylated recombinant human interleukin-10 (AM0010) in patients with advanced solid tumors. J. Clin. Oncol 34, 3562–3569. [PubMed: 27528724]

Nehete PN, Nehete BP, Hill L, Manuri PR, Baladandayuthapani V, Feng L, Simmons J, and Sastry KJ (2008). Selective induction of cell-mediated immunity and protection of rhesus macaques from chronic SHIV(KU2) infection by prophylactic vaccination with a conserved HIV-1 envelope peptide-cocktail. Virology 370, 130–141. [PubMed: 17920095]

Nizard M, Roussel H, Diniz MO, Karaki S, Tran T, Voron T, Dransart E, Sandoval F, Riquet M, Rance B, et al. (2017). Induction of resident memory T cells enhances the efficacy of cancer vaccine. Nat. Commun 8, 15221. [PubMed: 28537262]

Park H, Adamson L, Ha T, Mullen K, Hagen SI, Nogueron A, Sylwester AW, Axthelm MK, Legasse A, Piatak M Jr., et al. (2013). Polyinosinicpolycytidylic acid is the most effective TLR adjuvant for SIV Gag protein-induced T cell responses in nonhuman primates. J. Immunol 190, 4103–4115. [PubMed: 23509365]

Pichyangkul S, Yongvanitchit K, Limsalakpetch A, Kum-Arb U, Im-Erbsin R, Boonnak K, Thitithayanont A, Jongkaewwattana A, Wiboon-ut S, Mongkolsirichaikul D, et al. (2015). Tissue distribution of memory T and B cells in rhesus monkeys following infiuenza A infection. J. Immunol 195, 4378–4386. [PubMed: 26408671]

Pizzolla A, Nguyen THO, Smith JM, Brooks AG, Kedzieska K, Heath WR, Reading PC, and Wakim LM (2017). Resident memory $CD8^+$ T cells in the upper respiratory tract prevent pulmonary infiuenza virus infection. Sci. Immunol 2, 2.

Savas P, Virassamy B, Ye C, Salim A, Mintoff CP, Caramia F, Salgado R, Byrne DJ, Teo ZL, Dushyanthen S, et al. (2018). Single-cell profiling of breast cancer T cells reveals a tissue-resident memory subset associated with improved prognosis. Nat. Med 24, 986–993. [PubMed: 29942092]

Schenkel JM, Fraser KA, Vezys V, and Masopust D (2013). Sensing and alarm function of resident memory $CD8^+$ T cells. Nat. Immunol 14, 509–513. [PubMed: 23542740]

Slütter B, Van Braeckel-Budimir N, Abboud G, Varga SM, Salek-Ardakani S, and Harty JT (2017). Dynamics of infiuenza-induced lung-resident memory T cells underlie waning heterosubtypic immunity. Sci. Immunol 2, eaam6970. [PubMed: 28783656]

Thompson EA, Liang F, Lindgren G, Sandgren KJ, Quinn KM, Darrah PA, Koup RA, Seder RA, Kedl RM, and Loré K (2015). Human anti-CD40 antibody and poly IC:LC adjuvant combination induces potent T cell responses in the lung of nonhuman primates. J. Immunol 195, 1015–1024. [PubMed: 26123354]

von Haehling S, Wolk K, Höfiich C, Kunz S, Grünberg BH, Döcke WD, Reineke U, Asadullah K, Sterry W, Volk HD, and Sabat R (2015). Interleukin-10 receptor-1 expression in monocyte-derived antigen-presenting cell populations: dendritic cells partially escape from IL-10's inhibitory mechanisms. Genes Immun. 16, 8–14. [PubMed: 25472783]

Vono M, Lin A, Norrby-Teglund A, Koup RA, Liang F, and Loré K (2017). Neutrophils acquire the capacity for antigen presentation to memory $CD4^+$ T cells in vitro and ex vivo. Blood 129, 1991–2001. [PubMed: 28143882]

Yu CI, Becker C, Wang Y, Marches F, Helft J, Leboeuf M, Anguiano E, Pourpe S, Goller K, Pascual V, et al. (2013). Human CD1c+ dendritic cells drive the differentiation of CD103+ CD8+ mucosal effector T cells via the cytokine TGF-β. Immunity 38, 818–830. [PubMed: 23562160]

Highlights

- Intravenous administration of an agonistic anti-CD40 antibody induces early IL-10
- IL-10 levels in the plasma correlate with $CD103^+$ T_{RM}s in the lung
- Blocking IL-10 *in vitro* or *in vivo* reduces $CD103^+$ T_{RM}s
- Monocyte-derived IL-10 induces TGF-β release and CD103 upregulation on naive T cells

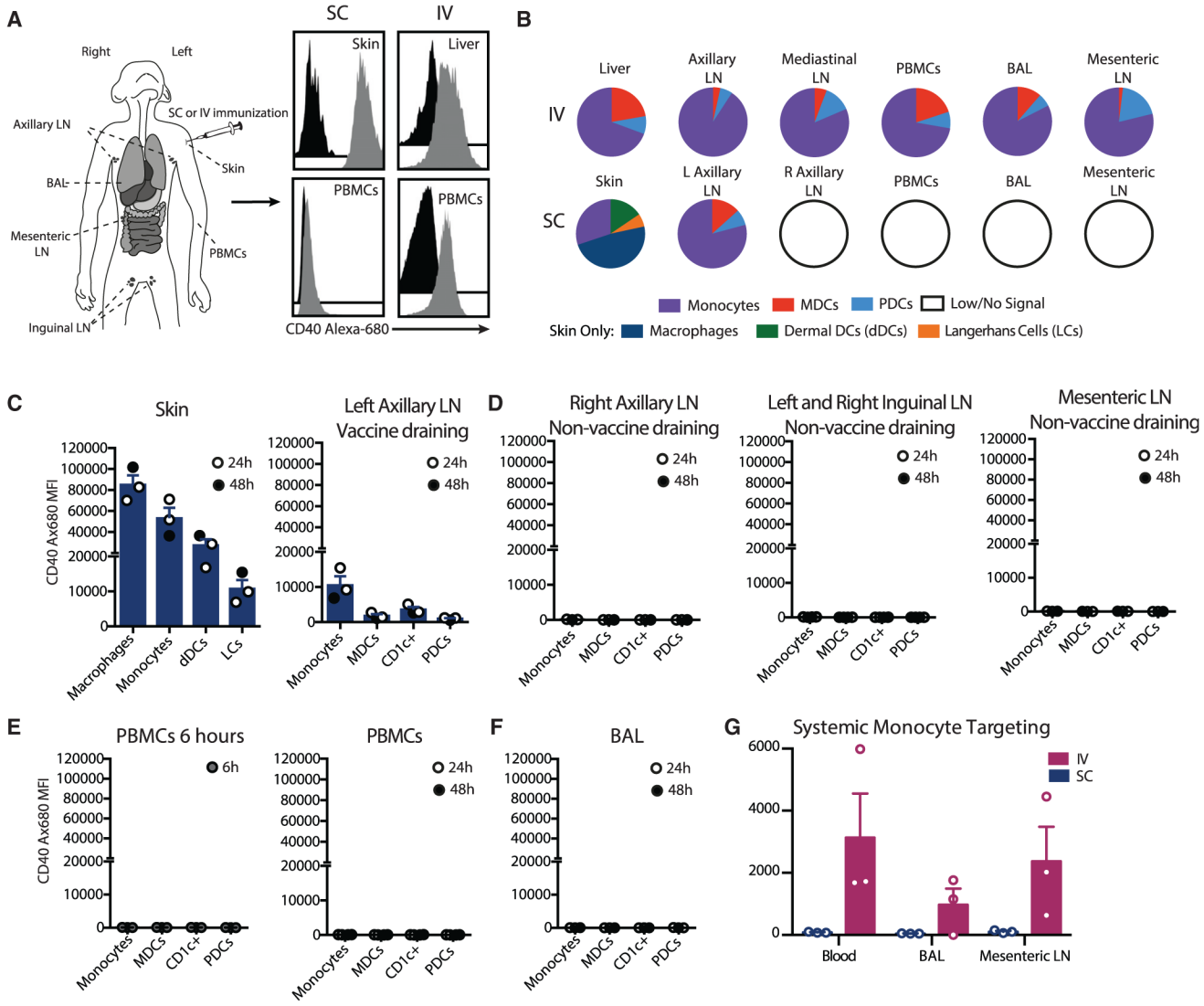

Figure 1. Local APC Targeting with Anti-CD40Ab following Subcutaneous Administration

(A) Rhesus macaques were immunized subcutaneously or i.v. with Alexa-Fluor-680-labeled anti-CD40Ab and poly(IC:LC). For s.c. immunization, indicated samples were collected at 24 and 48 h. Shown are representative histograms of the monocyte Alexa Fluor 680 signal from immunized (gray) or unimmunized (black) animals.

(B) Proportion of the CD40 Alexa Fluor 680 signal (mean fluorescent intensity, MFI) of APCs in collected tissues.

(C–F) CD40 Alexa Fluor 680 MFI on APCs.

(G) Monocyte binding following s.c. or i.v. administration. Each data point represents a separate animal (n = 3, mean ± SEM). See also Figure S1.

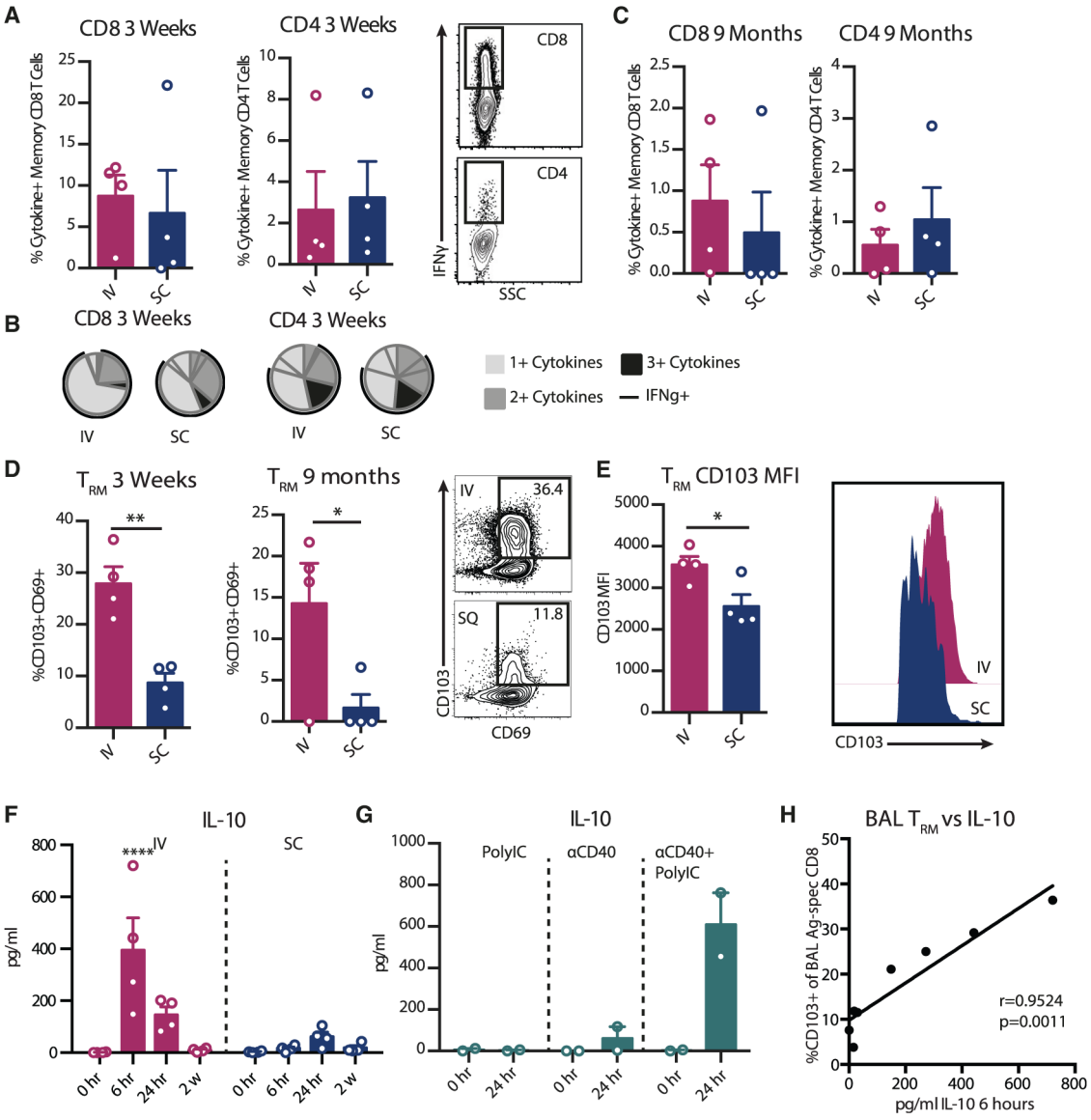

Figure 2. Differential T_{RM} Phenotype after i.v. and s.c. Vaccine Administration Correlates with IL-10 Production

Rhesus macaques were immunized with Env peptides, anti-CD40Ab, and poly(IC:LC) (n = 4/group). BAL samples were stimulated overnight with an immunizing peptide pool to recall total memory Ag-specific T cells ($CCR7^+CD45RA^+$ naive T cells excluded, producing interferon-γ (IFN-γ), IL-2, or tumor necrosis factor [TNF]).

(A–C) Frequency of Ag-specific CD8 or CD4 T cells 3 weeks (A) and 9 months (C) post-immunization. (B) Proportion of multifunctional T cells at 3 weeks.

(D) Frequency of $CD103^+CD69^+$ T_{RM}s of Ag-specific CD8 T cells.

(E) MFI of CD103 expression on Ag-specific T_{RM}s at 3 weeks.

(F) IL-10 levels in plasma.

(G) IL-10 levels in plasma after i.v. administration of Poly IC:LC, anti-CD40, or the combination (n = 2/group).

(H) Correlation of frequency of TRM of Ag-specific CD8 T cells in BAL at 3 weeks (y axis) with IL-10 (pg/mL) in plasma at 6 h (x axis). Each data point represents a separate animal (mean ± SEM).

Significance was tested using an unpaired Student's t test (A–E), one-way ANOVA (F), or Spearman's test (H). See also Figure S2.

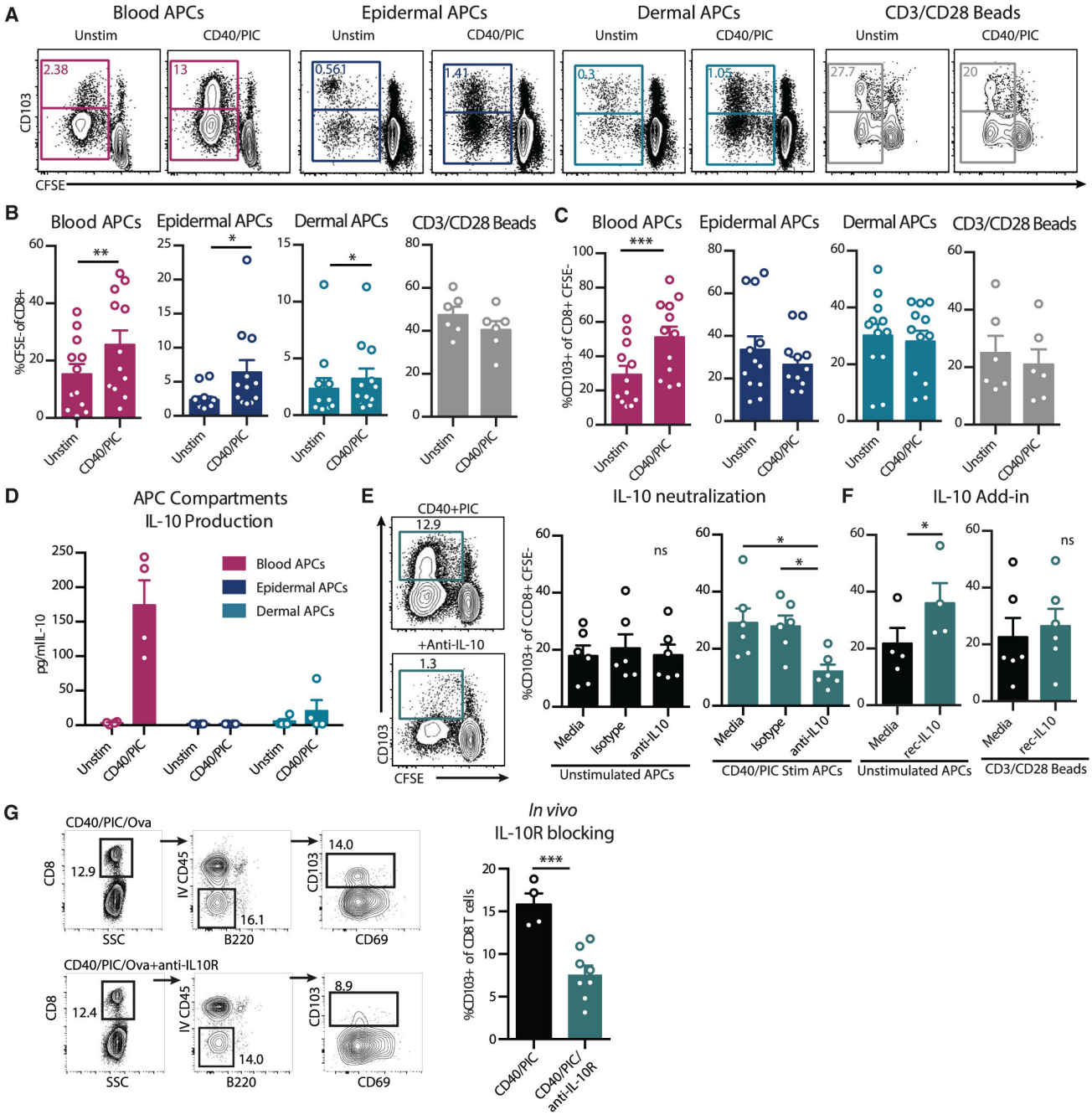

Figure 3. APC Stimulation Induces T_{RM} Differentiation via IL-10

(A–C) APC-enriched blood, epidermal APCs, or dermal APCs were cultured with CFSE-labeled allogenic naive T cells for 6 days, with or without prestimulation with anti-CD40Ab and poly(I:C) (CD40/PIC) (n = 12). T cells were cultured with anti-CD3-CD28 stimulation beads as a control (n = 6). (A) Representative flow plot of CFSE dilution and CD103 expression. (B) CD8 T cell proliferation as assessed by %CFSE low. (C) Frequency of proliferating CD8 T cells expressing CD103.

(D) IL-10 levels in supernatants from overnight stimulated APC cultures (n = 4).

(E and F) Co-cultures were supplemented with a neutralizing anti-IL-10 Ab or isotype control (E) or recombinant IL-10 (F). Frequency of proliferating CD8 T cells expressing CD103 is shown. Each data point represents a separate human donor (n = 4–6).
(G) Wild-type C57BL6 mice were immunized i.v. with ova, poly(I:C), and anti-CD40, with or without intraperitoneal (i.p.) injection of anti-IL10R blocking Ab 4 h prior to immunization. Lung-resident extravascular T cells were identified by i.v. injection of anti-CD45. Shown are representative flow plots and summary of %$CD103^+$ of CD8 T cells. Each dot represents a separate mouse (n = 4–8, mean ± SEM).
Significance was tested using an unpaired Student's t test (B, C, F, and G) or one-way ANOVA (E). See also Figure S3.

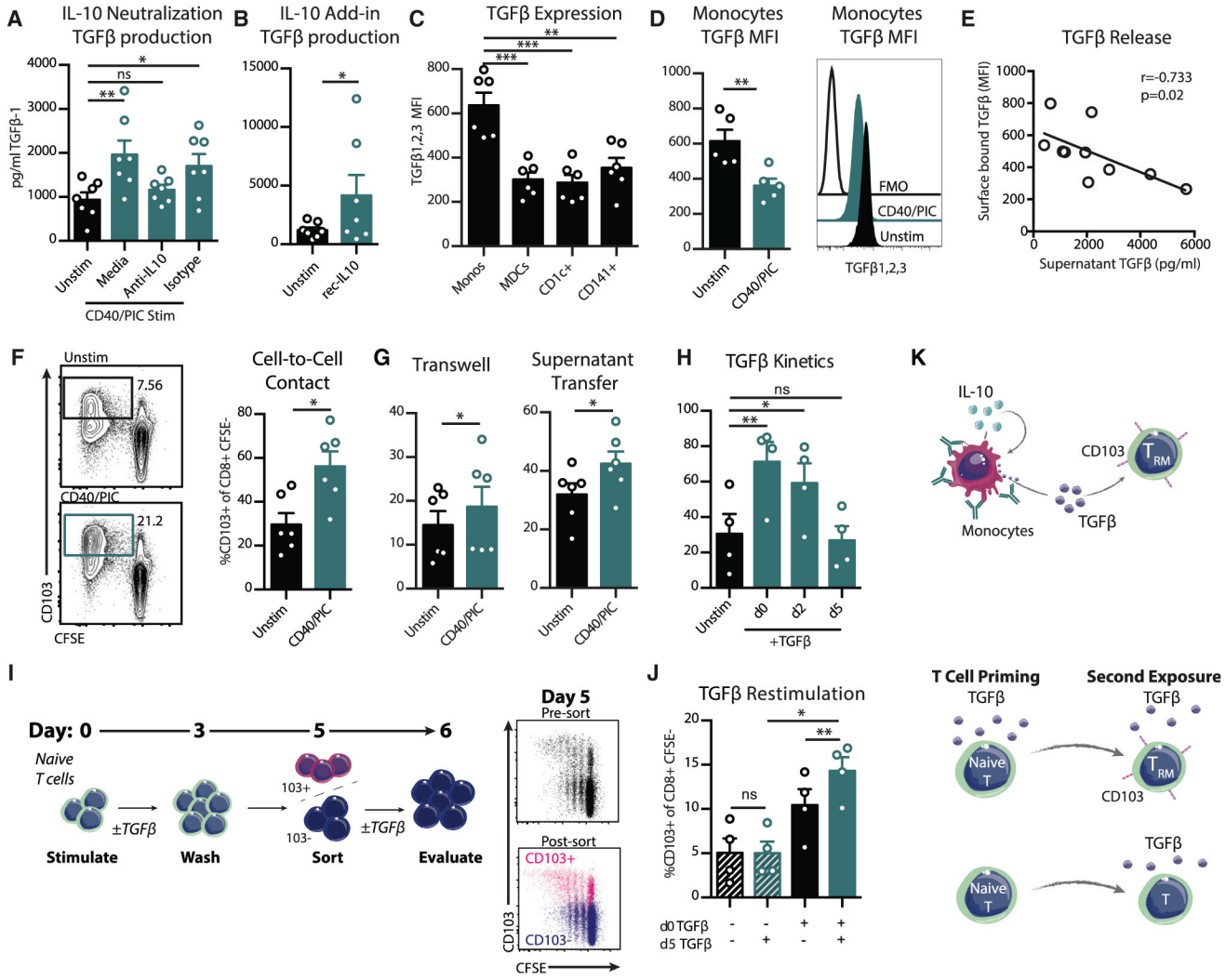

Figure 4. IL-10 Stimulates the Release of Monocyte TGF-β and T_{RM} Priming

(A and B) TGF-β1 levels in supernatants of stimulated blood APC cultures after 6 h with anti-IL10 (A) or recombinant IL-10 (B) (n = 7). (C and D) Surface expression of TGF-β1, TGF-β2, and TGF-β3 after 6 h in culture unstimulated (C) or stimulated (D) (n = 6).

(E) Correlation of secreted TGF-β1 (x axis) and monocyte TGF-β MFI (y axis) (n = 5).

(F) Purified $CD14^+$ monocytes were cultured with CFSE-labeled allogenic naive T cells (n = 6).

(G) Purified $CD14^+$ monocytes were cultured in a transwell assay with CFSE-labeled naive T cells stimulated with CD3-CD28 beads, or supernatants were transferred from monocytes after overnight stimulation. Frequency of proliferating CD8 T cells expressing CD103 is shown (n = 6).

(H–J) Naive CFSE-labeled T cells were stimulated with CD3-CD28 beads (n = 4). (H) Cultures were supplemented with TGF-β1 on day 0, 2, or 5 of the culture and evaluated for CD103 on day 6. (I) Experimental setup. T cells were cultured in the presence or absence of TGF-β1. Cells were washed on day 3 with fresh media and sorted for $CD103^-$ cells on day 5. $CD103^-$ cells were restimulated with TGF-β1 and evaluated for CD103 expression on day

6. Shown are representative plots of CD103 sorting purity of $CD103^+$ (pink) and $CD103^-$ (blue) fractions on day 5 and (J) summary of CD103 expression on day 6 of cultures. Each data point represents a separate human donor (mean ± SEM).

(K) Graphical summary of findings.

Significance was tested using an unpaired Student's t test (B, D, F, and G), one-way ANOVA (A, C, H, and J), or Spearman's test (E). See also Figure S4.

KEY RESOURCES TABLE

REAGENT or RESOURCE	SOURCE	IDENTIFIER
Antibodies		
BDCA1 FITC AD5–8E7	Miltenyi	130-113-301, RRID:AB_2726080
CCR7 BV421 G043H7	Biolegend	353208
CD103 APC 2G5	Beckman Coulter	B06204
CD11c Cy7PE 3.9	Biolegend	301608
CD123 PercP Cy55 7G3	BD	558714, RRID:AB_558714
CD141 VioBlue AD5–14H12	Miltenyi	130-113-882, RRID:AB_2726374
CD1a PE SK9	BD	341641, RRID:AB_2073291
CD1c APC AD5–8E7	Miltenyi	130-110-537, RRID:AB_2656040
CD20 Cy7APC L27	BD	335829
CD209 PerCP Cy55 DCN46	BD	558263, RRID:AB_647256
CD3 Cy7 APC SP34–2	BD	557757, RRID:AB_396863
CD4 BV605 L200	BD	562843, RRID:AB_2737833
CD40 FITC 5C3	Biolegend	334306, RRID:AB_1186034
CD45 BV605 HI30	BD	564048
CD45 BV605 D058–1283	BD	564098
CD45RA Cy7PE L48	BD	649457, RRID:AB_10894017
CD69 Cy5PE FN50	BioLegend	310908
CD8 PE RPA-T8	BD	561950
HLA-DR Cy55PE Tü36	Thermo Fisher	MHLDR18, RRID:AB_10372966
IFNg FITC B27	BD	554700, RRID:AB_395517
IL-10 APC JES3–19F1	BD	554707
IL2 BV605 MQ1–17H12	BioLegend	500332
TGFb1,2,3 AF700 1D11	R&D	IC1835N
TNFa BV650 MAb11	Biolegend	502938
Purified Rat Anti-Human IL-10 JES3-	BD	554704, RRID:AB_398581
mAb anti-mouse IL-10R (CD210)	BioXcell	BE0050, RRID:AB_1107611
Chemicals, Peptides, and Recombinant Proteins		
Anti-CD40 clone 341G2	Aragen Biosciences	Lot#: AB120830–1
Poly I:C	Invivogen	Tlrl-pic
HIV-ENV Peptides	Biomatik	Custom synthesis
Recombinant IL-10	Peprotech	200–10
Critical Commercial Assays		
Alexa Fluor 680 Antibody Labeling Kit	Thermo Fisher	A20188
Human IL-10 ELISA pro kit	Mabtech	3430–1HP-2
NHP Luminex Custom kit	EMD Millipore	PRCYTOMAG-40K-11
Human TGF-beta 1 Quantikine ELISA Kit	R&D	DB100B
Monocyte Rosettesep Enrichment kit (custom)	StemCell Technologies	15309
IL-10 Secretion Assay	Miltenyi	130-090-435
Naive Pan T Cell Isolation Kit, human	Miltenyi	130-097-095

REAGENT or RESOURCE	SOURCE	IDENTIFIER
T Cell Activation/Expansion Kit, human	Miltenyi	130-091-441
Experimental Models: Organisms/Strains		
C57BL/6J	Jackson Laboratory	000664
Rhesus Macaque	PrimGen, PreLabs	N/A